Journal of Achievements in Materials and Manufacturing Engineering
VOLUME 50
ISSUE 2
February
2012

Mössbauer investigations of amorphous $Fe_{(80-x)}B_{20}Nb_x$ (x=0,4,6,10) alloys

R. Babilas [a,*], R. Nowosielski [a], M. Kądziołka-Gaweł [b], A. Zajączkowski [c]
[a] Institute of Engineering Materials and Biomaterials, Silesian University of Technology, ul. Konarskiego 18a, 44-100 Gliwice, Poland
[b] Institute of Physics, University of Silesia, ul. Uniwersytecka 4, 40-007 Katowice, Poland
[c] Institute of Non-Ferrous Metals, ul. Sowińskiego 5, 44-100 Gliwice, Poland
* Corresponding e-mail address: rafal.babilas@polsl.pl

Received 12.12.2011; published in revised form 01.02.2012

Materials

ABSTRACT

Purpose: The paper presents a structural and magnetic characterization of selected Fe-based metallic glasses in as-cast state.

Design/methodology/approach: The studies were performed on $Fe_{(80-x)}B_{20}Nb_x$ metallic glasses in form of ribbons with Nb addition of 0, 4, 6, 10 at.%. The amorphous structure of tested samples was examined by X-ray diffraction (XRD) and Mössbauer spectroscopy methods. The Mössbauer spectroscopy was also applied to comparison of structure in studied amorphous samples with different chemical composition. The thermal properties associated with solidus temperature of master alloys were measured using the differential thermal analysis (DTA). The soft magnetic properties examination of tested materials contained relative magnetic permeability.

Findings: The XRD and Mössbauer spectroscopy investigations revealed that the studied alloys in as-cast state were amorphous. The solidus temperature assumed as the onset temperature of the melting peak on the DTA curve reached a value of 1405, 1394, 1392 and 1389 K for $Fe_{80}B_{20}$, $Fe_{76}B_{20}Nb_4$, $Fe_{74}B_{20}Nb_6$ and $Fe_{70}B_{20}Nb_{10}$ alloy, adequately. The Mössbauer spectra presented broadened six line patterns characteristic to the structural disorder of amorphous ferromagnetic materials. The changing of the average hyperfine magnetic field with niobium addition is connected with structural changing. A high concentration of Nb atoms with high atomic radius can acting as diffusion barrier what lead to formation of regions rich in iron or boron atoms. The niobium addition in $Fe_{(80-x)}B_{20}Nb_x$ alloy improves soft magnetic properties in as-cast state.

Practical implications: The Mössbauer spectroscopy is very useful method in studying the structural environment of Fe atoms on a nearest-neighbor length scale allowing the analysis of iron-containing phases.

Originality/value: The obtained examination results confirm the utility of investigation methods in analysis of microstructure of ferromagnetic glassy alloys.

Keywords: Amorphous materials; Fe-based metallic glasses; Mössbauer spectroscopy; Thermal analysis

Reference to this paper should be given in the following way:
R. Babilas, R. Nowosielski, M. Kądziołka-Gaweł, A. Zajączkowski, Mössbauer investigations of amorphous $Fe_{(80-x)}B_{20}Nb_x$ (x=0,4,6,10) alloys, Journal of Achievements in Materials and Manufacturing Engineering 50/2 (2012) 66-73.

1. Introduction

The ferromagnetic amorphous alloys have been studied due to the attractive properties for soft magnetic applications. The required magnetic properties are usually large saturation magnetization, low coercive field and high permeability [1-3].

First Fe-based metallic glasses synthesized by Duwez in 1967 exhibiting good physical, chemical properties and corrosion resistance. In case to improve its physical properties a lot of different alloying elements, in different concentration replacing Fe, have been added to the system during the preparation of the glassy materials [4-7].

It is known that Fe-based metallic glasses exhibit soft magnetic properties better than those corresponding to the crystalline alloys, but their preparation requires high critical cooling rates of about 10^6 K/s. This condition limits the size of the magnetic elements, which can be cast in the form of sheets, ribbons, wires or thin films with reduced dimensions [8].

However, Inoue et al. achieved some Fe-based bulk amorphous and nanocrystalline alloys in [1,9-11]:

a) Fe-(Al,Ga)-P-C-B,
b) Fe-Co-Ln-B;
c) Fe-(Co,Ni)-B-Si-Nb;
d) Fe-Co-Zr-Mo-W-B
e) Fe-(Co, Ni)-(Zr, Hf, Nb, Ta)-B;
f) Fe-(Cr,Mo)-(P,B,C);
g) Fe-(Zr,Hf,Nb)-B;

alloy systems, which combine a large glass-forming ability with good soft magnetic properties. These alloys can be prepared in ribbon shape (thickness up to 200 μm) or in the form of rods (diameter up to few millimeters) with critical cooling rates up to 1 K/s [2].

Inoue formulated three empirical principles to develop alloys with high glass-forming ability. Firstly, the system must contain more than three elements, secondly the difference of atomic sizes among the main constituent elements must be larger than 12%, and thirdly the heats of mixing among the constituent elements must be large negative values. In addition, it could be said that system should be eutectic [1-3,9].

The bulk amorphous alloys with enhanced dimension without crystallization of the samples are very attractive materials for industrial mass production. Good soft magnetic properties are another interesting feature of that can be used in applications. The amorphous state of metallic glasses is associated with a high degree of dense random-packed structure, a new local atomic configuration that is different from those for the crystalline alloys and a long-range atomic configuration [1,8,9,12].

Minor changes of chemical composition of metallic-glasses may caused significant changes of their glass-forming ability and physical properties such as strength, ductility, corrosion resistance or magnetic properties. The alloying addition of some element modifies the liquid structure by changing the atomic packing configuration and forming strong bonds with other elements. In this case viscosity is increased, which caused the decreasing of atomic arrangement necessary for crystallization process [13].

The addition of Nb, Ta and Mo to the Fe-Co system is expected to improve its thermal stability. The combination of these alloying additions in boron rich alloys is important for forming bulk metallic glasses [14].

The paper presents the influence of Nb addition on structure and magnetic properties of $Fe_{(80-x)}B_{20}Nb_x$ amorphous alloys in as-cast state. In order to achieve good thermal properties as wide supercooled liquid region and phase stability until high temperature, the purpose of paper is concentrated on studies of alloys with higher content of niobium.

Moreover, Mössbauer spectroscopy was used to investigate the local structure and magnetic behavior for studied metallic glasses, because Mössbauer spectroscopy is sensitive to the chemical and structural environment of the iron atoms on a nearest-neighbor length scale [6,15].

Combination of X-ray diffraction and Mössbauer spectroscopy methods gives better structural information of amorphous materials. It is important to note that X-ray diffraction can not differentiate between kind of atoms and their scattering amplitudes are very similar [12].

The XRD method gives information about the average pair correlation function. However, Mössbauer spectroscopy method is able to resolve the different kinds of Fe atoms and provide information about the local environment around Fe atoms. Moreover, the hyperfine field is more sensitive to the boron near neighbour and it gives information about the variations in the metalloid near-neighbour environment [16].

2. Material and research methodology

The aim of the this paper is the local structure analysis of $Fe_{(80-x)}B_{20}Nb_x$ (x = 0, 4, 6, 10) metallic glasses in as-cast state using XRD, DTA, Mössbauer spectroscopy and magnetic examination methods.

The ingot of Fe-based master alloys were prepared by induction melting of a mixture of pure elements of Fe, Nb and B under argon protective gas atmosphere. Investigations were done on binary alloy with composition of $Fe_{80}B_{20}$ and ternary alloys with different Nb addition (4, 6, 10 at.%) and composition of $Fe_{76}B_{20}Nb_4$, $Fe_{74}B_{20}Nb_6$, $Fe_{70}B_{20}Nb_{10}$ for comparison.

The previous prepared master alloy was cast as ribbon shaped metallic glasses with thickness of 0.05 mm and with of 2 mm. The ribbons were manufactured by the “chill-block melt spinning” (CBMS) technique, which is a method of continuous casting of the liquid alloy on the turning copper wheel [17-27].

The casting conditions include linear speed of copper wheel of 20 m/s and ejection over-pressure of molten alloy under argon atmosphere of 0.02-0.04 MPa.

Structure analysis of the samples was carried out using X-ray diffractometer (XRD) with $Co_{K\alpha}$ radiation. The data of diffraction lines were recorded by “step-scanning” method in 2θ range from 30° to 90° for samples in as-cast state.

The solidus temperature of studied Fe-based master alloys were measured using the differential thermal analysis (DTA) at a constant heating rate of 6 K/s under an argon protective atmosphere.

Magnetic measurements of studied ribbons, carried at room temperature, included relative magnetic permeability (μ_r) [28-30] - determined by E4980A Agilent LCR Meter at a frequency of 1030 Hz and magnetic field up to $H = 100$ A/m;

The Fe^{57} Mössbauer spectra were recorded in a room temperature using a constant acceleration spectrometer with Co57:Pd source. Metallic iron powder was used for velocity calibrations of the Mössbauer spectrometer [31].

All spectra were fitted by means of a hyperfine field distribution using the Hesse-Rübartsch procedure [32] with linear correlation between isomer shift an hyperfine magnetic field and an elementary line width 0.17 mm/s.

3. Results and discussion

The amorphous structure of Fe-based alloys cast in form of ribbons was firstly examined by X-ray diffraction method. Figures 1, 3, 5 and 7 presents the XRD investigations for $Fe_{80}B_{20}$, $Fe_{76}B_{20}Nb_4$, $Fe_{74}B_{20}Nb_6$ and $Fe_{70}B_{20}Nb_{10}$ alloy, adequately. The diffraction patterns of studied ribbons in as-cast state show the broad diffraction halo for each sample, which is characteristic for the amorphous materials with disordered atomic structure.

Comparison of diffraction patterns of studied samples with different chemical composition (Nb addition in alloy) shows the slightly changing of diffraction lines. These results may indicate that different concentration of niobium caused structural changes of tested amorphous alloys.

The solidus temperature (T_m) and temperature of the end of melting process (T_l) assumed to be the onset and end temperature of the melting peak on the DTA (at 6 K/min) curves are presented in Figures 2, 4, 6 and 8.

The endothermic peak observed on DTA curve of master alloy of $Fe_{80}B_{20}$ composition allowed to determine the solidus temperature (T_m), which has a value of 1405 K and temperature of the end of melting process (T_l = 1543 K). In the similar way the endothermic effect was also observed for ingot of ternary alloys with Nb addition. The solidus temperature (T_m) reached a value of 1394 K and temperature of the end of melting process (T_l) obtained a value of 1472 K for $Fe_{76}B_{20}Nb_4$ and T_m = 1392 K, T_l = 1450 K for $Fe_{74}B_{20}Nb_6$ alloy, similarly. The fourth alloy ($Fe_{70}B_{20}Nb_{10}$) had the solidus temperature with a value of 1389 K and T_l temperature of 1466 K.

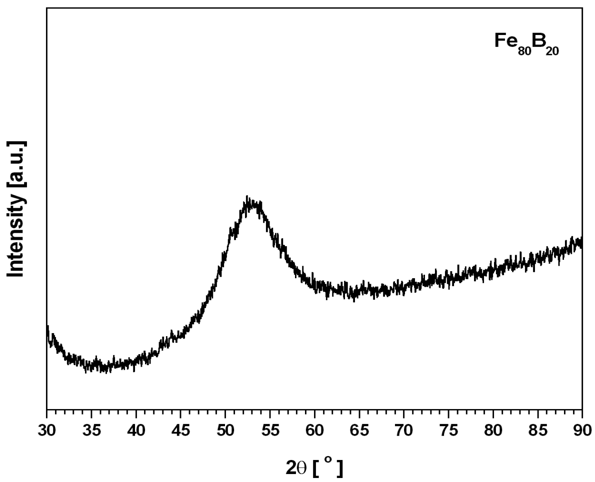

Fig. 1. X-ray diffraction pattern of $Fe_{80}B_{20}$ metallic glass in as-cast state in form of ribbon

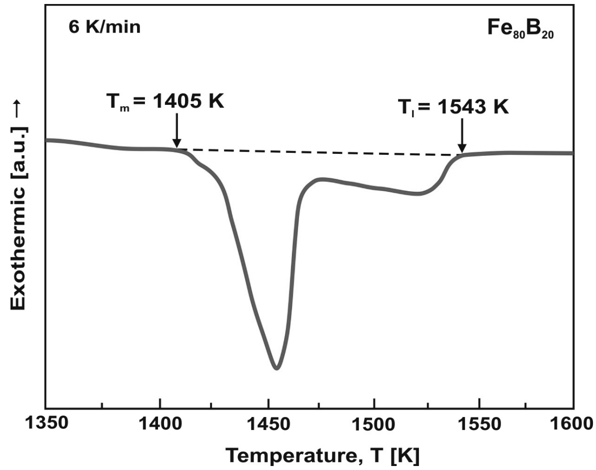

Fig. 2. DTA curve of $Fe_{80}B_{20}$ alloy as master-alloy

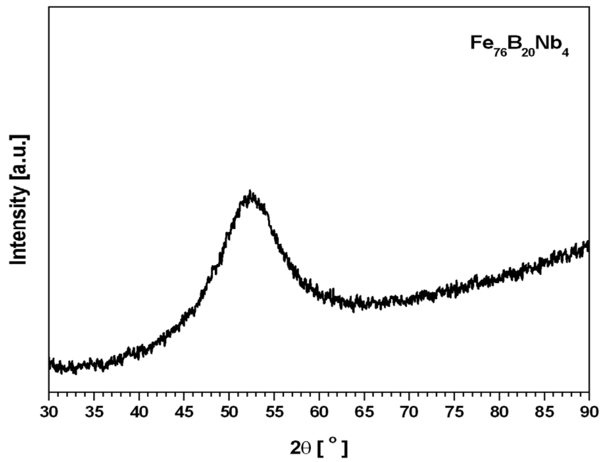

Fig. 3. X-ray diffraction pattern of $Fe_{76}B_{20}Nb_4$ metallic glass in as-cast state in form of ribbon

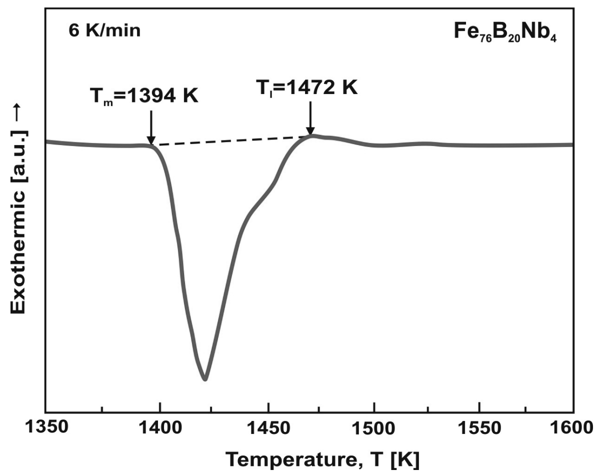

Fig. 4. DTA curve of $Fe_{76}B_{20}Nb_4$ alloy as master-alloy

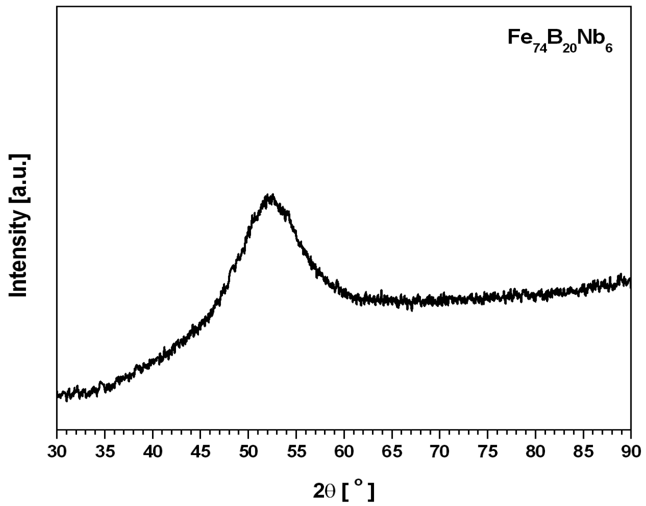

Fig. 5. X-ray diffraction pattern of $Fe_{74}B_{20}Nb_6$ metallic glass in as-cast state in form of ribbon

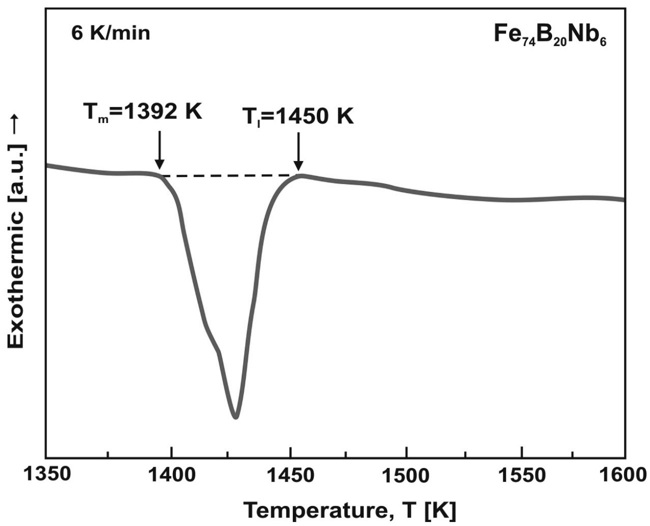

Fig. 6. DTA curve of $Fe_{74}B_{20}Nb_6$ alloy as master-alloy

In addition to DTA analysis of master alloys Table 1 summarizes obtained values of solidus temperature (T_m) and temperature of the end of melting process (T_l) of studied materials. It could be generally said that the addition of Nb in $Fe_{(80-x)}B_{20}Nb_x$ alloy slightly decreases the solidus temperature.

Mössbauer spectroscopy was used to study hyperfine interactions of the metallic glass in as-cast state. The role of Nb in the amorphous process of a $Fe_{(80-x)}B_{20}Nb_x$ (x = 0, 4, 6, 10) alloy was investigated and the influence of Nb substitution on the hyperfine field distribution and isomer shift of amorphous Fe-B-Nb alloys. Figure 9 presents Mössbauer spectra of all analyzed samples. The corresponding hyperfine magnetic fields distributions p(B_{hf}) with decomposition into low and high field components by Gaussian distributions are presented in Figure 10. The values of the average hyperfine magnetic field (B_{hf}) as well as the isomer shift (*IS*) parameters obtained for the best fitting are listed in Table 2.

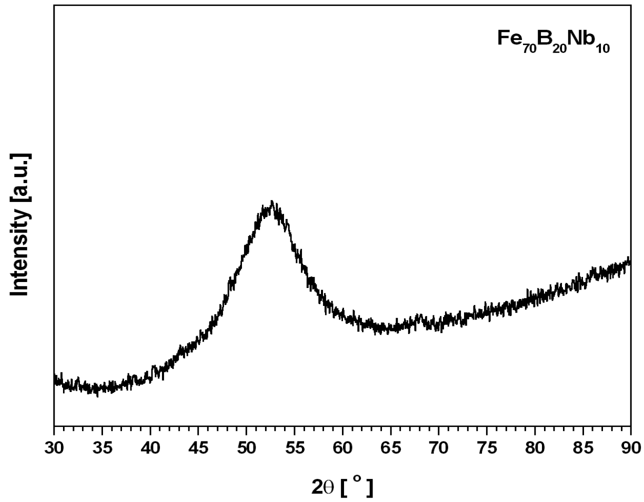

Fig. 7. X-ray diffraction pattern of $Fe_{70}B_{20}Nb_{10}$ metallic glass in as-cast state in form of ribbon

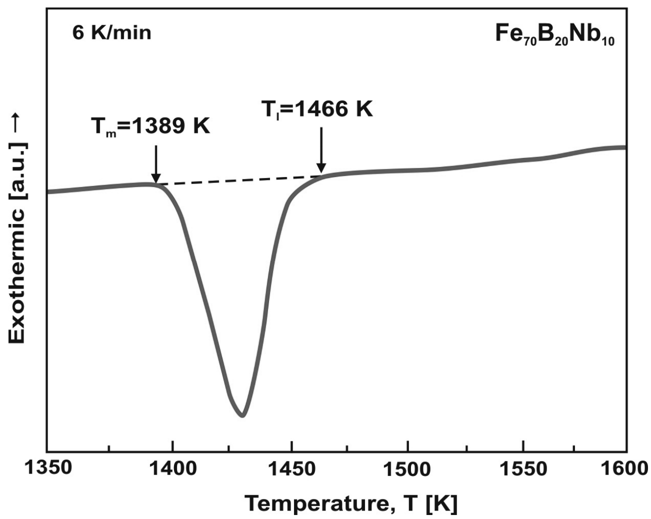

Fig. 8. DTA curve of $Fe_{70}B_{20}Nb_{10}$ alloy as master-alloy

Table 1.
Thermal properties of Fe80B20, Fe76B20Nb4, Fe74B20Nb6 and Fe70B20Nb10 master alloys

Master alloy	T_m [K]	T_l [K]
$Fe_{80}B_{20}$	1405	1543
$Fe_{76}B_{20}Nb_4$	1394	1472
$Fe_{74}B_{20}Nb_6$	1392	1450
$Fe_{70}B_{20}Nb_{10}$	1389	1466

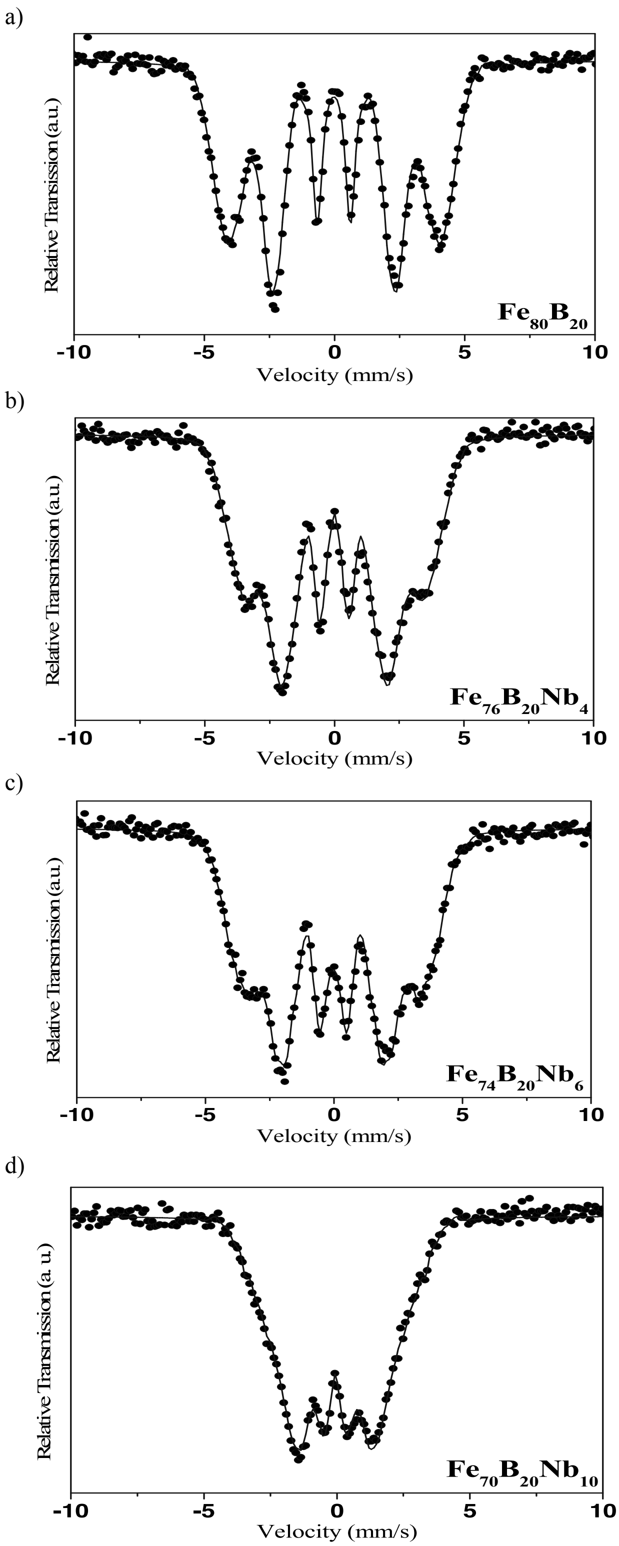

Fig. 9. Mössbauer spectra of: a) $Fe_{80}B_{20}$, b) $Fe_{76}B_{20}Nb_4$, c) $Fe_{74}B_{20}Nb_6$, d) $Fe_{70}B_{20}Nb_{10}$ metallic glasses in form of ribbon in as-cast state

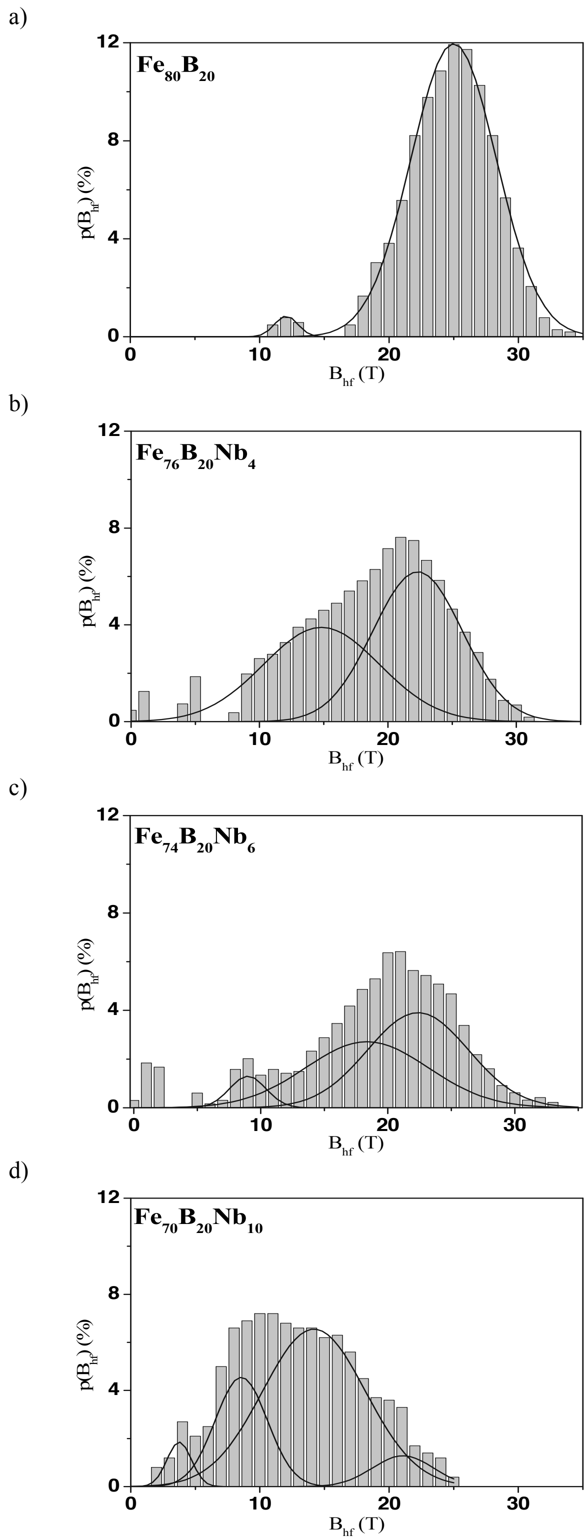

Fig. 10. Hyperfine field distribution of: a) $Fe_{80}B_{20}$, b) $Fe_{76}B_{20}Nb_4$, c) $Fe_{74}B_{20}Nb_6$, d) $Fe_{70}B_{20}Nb_{10}$ metallic glasses in form of ribbon in as-cast state

The shapes of the all spectra of investigated metallic glass samples are typical of amorphous ferromagnetic type materials. The hyperfine field distributions are broad. This is connected with different local surroundings of the Fe atom in investigated compounds what is characteristic for suchlike materials. The values of internal magnetic field B_{hf} depend upon the nearest neighbour distribution around Fe atoms, decreased as more Nb atoms surround Fe atoms. However, when Nb concentration is higher then 4 at.% on hyperfine magnetic field distributions are visible changes, some kind of segregation on low and high magnetic fields takes place. Probably, low fields, smaller then 15T, attributed to a Nb-rich environment amorphous phase [6]. The high magnetic fields, $B_{hf} > 15T$, are connected with presence of Fe-B environments [33]. Furthermore, it could be also stated that changing of the average hyperfine magnetic field with niobium addition is connected with structural changing occurred during casting the samples. It could lead the increase of the atom packing density, because of reducing free volumes.

Also, high concentration of Nb atoms with high atomic radius can acting as diffusion barrier what leads to formation of regions rich in iron or boron atoms. It is also confirmed by increasing of isomer shift and illustrated by growing number of Gaussian distributions. Basing on literature [34,35] low and high field components of p(B_{hf}) distributions could probably suggest the existing of different amorphous structures in studied materials. It is also possible that in amorphous matrix of $Fe_{(80-x)}B_{20}Nb_x$ alloys with (x > 4 at.%) may exist very small crystalline grains.

Table 2.
Average values of hyperfine magnetic field (Bhf) and isomer shift (IS) of $Fe_{(80-x)}B_{20}Nb_x$ metallic glasses in form of ribbons in as-cast state

Glassy alloy	B_{hf} [T]	*IS* [mm/s]
$Fe_{80}B_{20}$	24.6	0.071
$Fe_{76}B_{20}Nb_4$	18.6	0.092
$Fe_{74}B_{20}Nb_6$	18.8	0.075
$Fe_{70}B_{20}Nb_{10}$	16.7	0.034

Additionally, the relative magnetic permeability of the tested Fe-based alloys in relation to selected ribbons is shown in Figure 11. The applied magnetic field was up to 100 A/m.

Table 3.
The maximum magnetic permeability (μ_{rmax}) of studied $Fe_{(80-x)}B_{20}Nb_x$ metallic glasses in form of ribbons

Glassy alloy	μ_{rmax}
$Fe_{80}B_{20}$	1300
$Fe_{76}B_{20}Nb_4$	3400
$Fe_{74}B_{20}Nb_6$	4300
$Fe_{70}B_{20}Nb_{10}$	3015

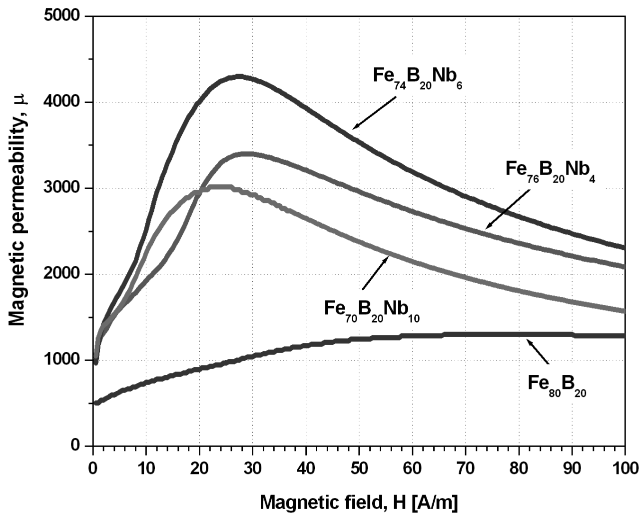

Fig. 11. Relative magnetic permeability of $Fe_{(80-x)}B_{20}Nb_x$ glassy ribbons in as-cast state

The maximum magnetic permeability (μ_{rmax}) for glassy ribbon of studied Fe-based alloys is changing with niobium addition. The μ_{rmax} has the highest value for alloy with composition of $Fe_{74}B_{20}Nb_6$ and reached a value of 4300. The basic alloy with composition of $Fe_{80}B_{20}$ has the lowest maximum magnetic permeability with value of 1300. The values of μ_{rmax} for remaining samples are presented in Table 3.

The niobium addition in $Fe_{(80-x)}B_{20}Nb_x$ alloy improves soft magnetic properties in as-cast state, especially with comparison with basic $Fe_{80}B_{20}$ binary alloy. This is a very good results, which allow to classify the studied Fe-based glassy alloy for suitable material for electric and magnetic applications.

4. Conclusions

The investigations performed on the samples of $Fe_{(80-x)}B_{20}Nb_x$ metallic glass allowed to formulate the following statements:

- the X-ray diffraction investigations revealed that the studied ribbons in as-cast state were amorphous,
- the shapes of the Mössbauer spectra of investigated metallic glass samples are typical for amorphous ferromagnetic materials,
- the measured shapes of the Mössbauer spectra and hyperfine fields distributions showed remarkable changes with niobium addition,
- the changing of the average hyperfine magnetic field with niobium addition is connected with structural changing, which leads to the increase of the atom packing density and reducing of free volume,
- increasing of Nb concentration leads to decreasing of average hyperfine magnetic field and isomer shift, which is illustrated by growing number of Gaussian distributions,
- high concentration of Nb atoms can acting as diffusion barrier what leads to formation of regions rich in iron or boron atoms what can lead to create very small crystalline regions,

- the solidus temperature assumed as the onset temperature of the melting peak on the DTA reached a value of 1405, 1394, 1392 and 1389 K for $Fe_{80}B_{20}$, $Fe_{76}B_{20}Nb_4$, $Fe_{74}B_{20}Nb_6$ and $Fe_{70}B_{20}Nb_{10}$ alloy, adequately,
- the niobium addition in $Fe_{(80-x)}B_{20}Nb_x$ alloy improves soft magnetic properties in as-cast state and decreases the solidus temperature.

References

[1] A. Inoue, K. Hashimoto, Amorphous and nanocrystalline materials: preparation, properties and applications, Springer, 2001.

[2] A. Inoue, A. Takeuchi, T. Zhang, Ferromagnetic bulk amorphous alloys, Metallurgical and Materials Transactions A 29/7 (1998) 1779-1793.

[3] A. Inoue, A. Makino, T. Mizushima, Ferromagnetic bulk glassy alloys, Journal of Magnetism and Magnetic Materials 215-216 (2000) 246-252.

[4] H.S. Chen, Glassy metals, Reports on Progress in Physics 43 (1980) 353-432.

[5] M.E. McHenry, M.A. Willard, D.E. Laughlin, Amorphous and nanocrystalline materials for applications as soft magnets, Progress in Materials Science 44 (1999) 291-433.

[6] J. Torrens-Serra, P. Bruna, J. Rodríguez-Viejo, T. Pradell, M.T. Clavaguera-Mora, Study of crystallization process of $Fe_{65}Nb_{10}B_{25}$ and $Fe_{70}Nb_{10}B_{20}$ glassy metals, Reviews on Advanced Materials Sciences 18 (2008) 464-468.

[7] K.G. Efthimiadis, K. Chrissafis, E.K. Polychroniadis, Combined study of crystallization of amorphous $Fe_{75-x}Ni_xSi_9B_{16}$ alloy, Materials Science and Engineering A 366 (2004) 211-220.

[8] A. Inoue, A. Takeuchi, Recent progress in bulk glassy, nanoquasicrystalline and nanocrystalline alloys, Materials Science and Engineering A 375-377 (2004) 16-30.

[9] W.H. Wang, C. Dong, C.H. Shek, Bulk metallic glasses, Materials Science and Engineering R 44 (2004) 45-89.

[10] A. Inoue, Bulk amorphous and nanocrystalline alloys with high functional properties, Materials Science and Engineering A 304-306 (2001) 1-10.

[11] A. Inoue, B.L. Shen, C.T. Chang, Fe- and Co-based bulk glassy alloys with ultrahigh strength of over 4000 MPa, Intermetallics 14 (2006) 936-944.

[12] S.N. Kane, A. Gupta, Zs. Gercsi, F. Mazaleyrat, L.K. Varga, Mössbauer and magnetic studies of $(Fe_{100-x}Co_x)_{62}Nb_8B_{30}$ (x=0,33,50) alloys, Journal of Magnetism and Magnetic Materials 292 (2005) 447-452.

[13] E. Pineda, P. Bruna, J. Serrano, J. Torrens-Serra, D. Crespo, Role of Mo in the local configuration and structure stabilization of amorphous steels, a Synchrotron X-ray diffraction and Mössbauer study, Journal of Alloys and Compounds 509 (2011) S56-S59.

[14] M. Sorescu, C.Y. Um, M.E. McHenry, L. Diamandescu, Thermal behavior of substituted FeCo-based metallic glasses, Journal of Non-Crystalline Solids 351 (2005) 663-667.

[15] D.Y. Liu, W.S. Sun, A.M. Wang, H.F. Zhang, Z.Q. Hu, Preparation, thermal stability, and magnetic properties of Fe-Co-Zr-Mo-W-B bulk metallic glass, Journal of Alloys and Compounds 370 (2004) 249-253.

[16] J.M. Greneche, Local structural order in disordered systems investigated by Mössbauer spectroscopy, Journal of Non-Crystalline Solids 287 (2001) 37-44.

[17] R. Nowosielski, R. Babilas, P. Ochin, Z. Stokłosa, Thermal and magnetic properties of selected Fe-based metallic glasses, Archives of Materials Science and Engineering 30/1 (2008) 13-16.

[18] R. Nowosielski, R. Babilas, Structure and properties of selected Fe-based metallic glasses, Journal of Achievements in Materials and Manufacturing Engineering 37/2 (2009) 332-339.

[19] R. Babilas, R. Nowosielski, Iron-based bulk amorphous alloys, Archives of Materials Science and Engineering 44/1 (2010) 5-27.

[20] S. Lesz, D. Szewieczek, J. Tyrlik-Held, Correlation between fracture morphology and mechanical properties of NANOPERM alloys, Archives of Materials Science and Engineering 29/2 (2008) 73-80.

[21] D. Szewieczek, J. Tyrlik-Held, S. Lesz, Structure and mechanical properties of amorphous $Fe_{84}Nb_7B_9$ alloy during crystallization, Journal of Achievements in Materials and Manufacturing Engineering 24 (2007) 87-90.

[22] D. Szewieczek, T. Raszka, Structure and magnetic properties of $Fe_{63.5}Co_{10}Cu_1Nb_3Si_{13.5}B_9$ alloy, Journal of Achievements in Materials and Manufacturing Engineering 18 (2006) 179-182.

[23] D. Szewieczek, T. Raszka, J. Olszewski, Optimisation the magnetic properties of the $(Fe_{1-x}Co_x)_{73.5}Cu_1Nb_3Si_{13.5}B_9$ (x=10; 30; 40) alloys, Journal of Achievements in Materials and Manufacturing Engineering 20 (2007) 31-36.

[24] S. Lesz, D. Szewieczek, J.E. Frąckowiak, Structure and magnetic properties of amorphous and nanocrystalline $Fe_{85.4}Hf_{1.4}B_{13.2}$ alloy, Journal of Achievements in Materials and Manufacturing Engineering 19 (2006) 29-34.

[25] L.A. Dobrzański, M. Drak, B. Ziębowicz, Materials with specific magnetic properties, Journal of Achievements in Materials and Manufacturing Engineering 17 (2006) 37-40.

[26] J. Konieczny, L.A. Dobrzański, J.E. Frąckowiak, Structure and properties of the powder obtained from the amorphous ribbon, Journal of Achievements in Materials and Manufacturing Engineering 18 (2006) 143-146.

[27] Ziębowicz, D. Szewieczek, L.A. Dobrzański, New possibilities of application of composite materials with soft magnetic properties, Journal of Achievements in Materials and Manufacturing Engineering 20 (2007) 207-210.

[28] Z. Stokłosa, G. Badura, P. Kwapuliński, J. Rasek, G. Haneczok, J. Lelątko, L. Pająk, Influence of alloying additions on enhancement of soft magnetic properties effect and crystallisation in FeXSiB (X=Cu, V, Co, Zr, Nb) amorphous alloys, Solid State Phenomena 130 (2007) 171-174.

[29] P. Kwapuliński, J. Rasek, Z. Stokłosa, G. Badura, B. Kostrubiec, G. Haneczok, Magnetic and mechanical properties in FeXSiB (X=Cu, Zr, Co) amorphous alloys, Archives of Materials Science and Engineering 31/1 (2008) 25-28.

[30] P. Kwapuliński, Z. Stokłosa, J. Rasek, G. Badura, G. Haneczok, L. Pająk, L. Lelątko, Influence of alloying

additions and annealing time on magnetic properties in amorphous alloys based on iron, Journal of Magnetism and Magnetic Materials 320 (2008) 778-782.
[31] R. Babilas, M. Kądziołka-Gaweł, R. Nowosielski, Structure studies of Fe-based metallic glasses by Mössbauer spectroscopy method, Journal of Achievements in Materials and Manufacturing Engineering 45/1 (2011) 7-12.
[32] J. Hesse, A. Rübartsch, Model independent evaluation of overlapped Mössbauer spectra, Journal of Physics E 7 (1974) 526-532.
[33] H. Franke, S. Dey, M. Rosenberg, F. E. Luborsky, J.L. Walter, Hyperfine fields and local magnetic moments of metallic glasses of 3d-transition metals, Journal of Magnetism and Magnetic Materials 15-18 (1980) 1364-1366.
[34] P. Pawlik, Soft magnetic Fe-Co-Zr-W-B bulk glassy alloys, Journal of Alloys and Compounds 423 (2006) 96-98.
[35] K. Brzózka, Structure and properties of iron based amorphous and nanocrystalline alloys investigated by mossbauer spectroscopy, Radom University of Technology Press, Radom, 2003 (in Polish).